

# Design of Thermally Reliable Environmental Barrier Coating for a SiC/SiC Ceramic Matrix Composites

E. K. Arthur<sup>1,\*</sup>, E. Ampaw<sup>1</sup>, S. T. Azeko<sup>1</sup>, Y. Danyuo<sup>1</sup>, B. Agyei-Tuffour<sup>1,2</sup>, K. Kan-Dapaah<sup>1,3</sup>,  
J. D. Obayemi<sup>1</sup>

<sup>1</sup>Department of Materials Science and Engineering, African University of Science and Technology, Abuja, Nigeria

<sup>2</sup>Department of Materials Science and Engineering, Private Mail Bag, University of Ghana, Legon, Accra, Ghana

<sup>3</sup>Department of Biomedical Engineering, Private Mail Bag, University of Ghana, Legon, Accra, Ghana

**Abstract** Silicon carbide-fiber-reinforced silicon carbide matrix composites (SiC/SiC CMCs) have been proven to possess greater high-temperature strength and durability. These materials are usually used in air breathing engines due to their unique properties. However, the application of SiC/SiC CMCs is ineffective in combustion environment due to oxidation and surface recession. Efforts to improve service of SiC/SiC CMCs in combustion environments require knowledge of their long-term stability in combustion environments, volatility, phase stability, and thermal conductivity. Therefore in this paper, the design of a reliable EBC for SiC/SiC CMCs with excellent corrosion, recession and thermal shock resistance is proposed. This design consists of a three-multilayer; yttrium disilicate/mullite/ytterbium disilicate ( $Y_2Si_2O_7/3Al_2O_3/2SiO_2/Yb_2Si_2O_7$ ) system. Also, finite element models (FEMs) were used to predict the thermal residual stresses within the proposed multilayers under operating conditions. The implications of the results are discussed for potential application of this EBC system in air breathing engines.

**Keywords** Yttrium Disilicate, Mullite, Ytterbium Disilicate, SiC/SiC CMCs, Environmental Barrier Coatings, FEM

## 1. Introduction

There have been significant efforts to develop silicon (Si)-based ceramics for air breathing engines in combustion environment[1]. This is due to their ability to handle high temperatures. There is no doubt that, the temperature capability of metallic structural components such as blades, nozzles, and combustor liners in hot engine section has become a major problem in the performance of gas turbines[2]. This has led to the development of ceramic matrix composites (CMCs). CMCs are possible candidates for various applications in high temperature environments with aggressive gases and possible corrosion deposits[1]. The hot section of most gas turbine engines can be made from Si-based ceramics such as silicon carbide - fiber - reinforced silicon carbide matrix composites (SiC/SiC CMCs) and monolithic silicon nitride ( $Si_3N_4$ )[3].

However, when the Si-based ceramic is exposed to corrosive environments containing high-pressure steam at elevated temperatures, they are susceptible to hot-corrosion and recession. The silica oxidation product formed from Si-containing materials further reacts with water vapor to

form  $Si(OH)_4$  (g)[1]. To mitigate the recession rates in air breathing silicon containing materials, environmental barrier coatings (EBCs) are needed. EBCs protect, SiC/SiC CMCs and other silicon containing materials from oxidation and recession. Among the factors considered for proper functioning of an EBC include phase stability of the coating with the substrate, e.g., SiC, and low coefficient of thermal expansion (CTE) with the substrate. The EBC should also have low permeability to oxygen, chemical compatibility with the silica scale formed from oxidation[4].

EBC design usually consists of two or more coating layers. Among the constituents of EBCs for SiC/SiC composites are Barium-Strontium-Alumino-Silicate (BSAS), rare earth mono- and di-silicates, and hafnia/zirconia based systems[3, 5, 6, 7]. Microstructure and durability of such coatings depend on the thickness and the processing methods used. Air plasma spray (APS), sputtering or slurry deposition and electron beam assisted physical vapor deposition are some of the common techniques for coating SiC/SiC turbine composites[8]. The first generation EBC consists of two layers; namely, mullite bond coat and yttria-stabilized zirconia (YSZ,  $ZrO_2 - 8 \text{ wt. } \% Y_2O_3$ ) top coat. Second generation EBCs with substantially improved performance consist of three layers, a silicon bond coat, a mullite or a mullite + BSAS ( $BaO_{1-x} - SrO_x - Al_2O_3 - 2SiO_2$ ) interlayer[9, 10] and a BSAS top coat.

Constant exposure of the EBCs to air breathing conditions

\* Corresponding author:

ekarthur2005@yahoo.com (E. K. Arthur)

Published online at <http://journal.sapub.org/cmaterials>

Copyright © 2013 Scientific & Academic Publishing. All Rights Reserved

introduces thermal residual stresses in the coating which eventually leads to the failure of the coatings[8]. Understanding the residual stresses[13] within the EBC multilayers enable the design of solutions to EBC failure.

In this paper, EBC design and two dimensional (2D) thermal residual stresses analyses of a reliable EBC for a SiC/SiC CMCs are discussed.

## 2. Materials and Methods

### 2.1. EBC Design and Architecture

The design considered a three multilayer EBC on SiC/SiC CMC. Each distinct layer performs a unique function(s). The first layer serves as a bond coat with SiC/SiC CMC, the intermediate layer helps to prevent oxidation, while the topcoat increases oxidation resistance and slows down SiO<sub>2</sub> volatilization as shown in Figure 1a.

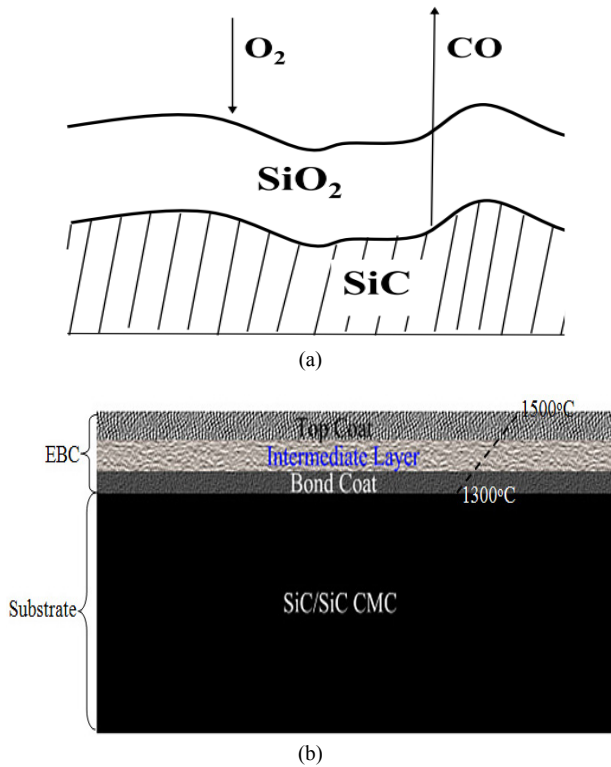


**Figure 1.** Schematic diagram of (a) surface recession of SiC and (b) SiC/SiC CMCs coated with three EBC multilayers

### 2.2. Environmental Barrier Coating: Materials Selection

**Table 2.** Physical, thermal, and mechanical properties of the proposed multilayers

Layers	CTE (°C)	Thermal Conductivity (W/m-K)	Heat Capacity (J/Kg.K)	Density (g/cm <sup>3</sup> )	Elastic Modulus (GPa)	Poisson's Ratio
Y <sub>2</sub> Si <sub>2</sub> O <sub>7</sub>	3.9 x 10 <sup>-6</sup> [12]	3.5 <sup>[13]</sup>	274*	3.96 <sup>[13]</sup>	155 <sup>[13]</sup>	0.27 <sup>[12]</sup>
3Al <sub>2</sub> O <sub>3</sub> .2SiO <sub>2</sub>	5.5x10 <sup>-6</sup> [14]	1.29 <sup>[15]</sup>	760 <sup>[15]</sup>	2.71 <sup>[15]</sup>	145 <sup>[14]</sup>	0.25 <sup>[16]</sup>
Yb <sub>2</sub> Si <sub>2</sub> O <sub>7</sub>	4.8x10 <sup>-6</sup> [9]	1.86 <sup>[17]</sup>	274*	6.19 <sup>[18]</sup>	90 <sup>[9]</sup>	0.18 <sup>[9]</sup>
SiC/SiC CMC	4.0x10 <sup>-6</sup> [19]	9.0 <sup>[19]</sup>	750 <sup>[19]</sup>	2.4 <sup>[19]</sup>	300 <sup>[19]</sup>	0.16 <sup>[19]</sup>

\*The heat capacities of Y<sub>2</sub>Si<sub>2</sub>O<sub>7</sub> and Yb<sub>2</sub>Si<sub>2</sub>O<sub>7</sub> were calculated using Dulong-Petit equation[17]

### 2.2.1. Oxide Layer Selection

In this paper, the choice of materials for the bond coat was based on the following factors; environmental stability, especially in water vapor, CTE match, and chemical compatibility with SiC/SiC. Based on the above factors, Y<sub>2</sub>Si<sub>2</sub>O<sub>7</sub>, Yb<sub>2</sub>Si<sub>2</sub>O<sub>7</sub> and 2Al<sub>2</sub>O<sub>3</sub>.3SiO<sub>2</sub> were selected as bond coat, top coat and intermediate layer respectively. Due to its similar low CTE to SiC ~ 4.0 x 10<sup>-6</sup>/°C[14], Y<sub>2</sub>Si<sub>2</sub>O<sub>7</sub> was chosen as bond coat material. To grade the CTE, mullite with CTE~ 5.5 x 10<sup>-6</sup>/°C[14] was selected as the intermediate layer to prevent oxidation. Yb<sub>2</sub>Si<sub>2</sub>O<sub>7</sub> (with CTE of 4.8x10<sup>-6</sup>/°C[9]) was finally chosen as the top coat to improve the oxidation resistance and also to minimize SiO<sub>2</sub> volatilization. The layer thicknesses were varied as shown in Table 1 and their corresponding thermal residual stresses were predicted using finite element modeling (FEM).

**Table 1.** Layer thickness used in the FEM

Layers	Model 1 Layer thickness	Model 2 Layer thickness	Model 3 Layer thickness
Y <sub>2</sub> Si <sub>2</sub> O <sub>7</sub>	200 μm	100 μm	100 μm
3Al <sub>2</sub> O <sub>3</sub> .2SiO <sub>2</sub>	200 μm	100 μm	200 μm
Yb <sub>2</sub> Si <sub>2</sub> O <sub>7</sub>	130 μm	100 μm	75 μm
SiC/SiC CMC	3 mm	3 mm	3 mm

### 2.3. FEM of Thermal Residual Stress

Thermo-mechanical simulations of the multilayer structure were performed using the Structural Mechanics Module and Heat Transfer Module of COMSOL Multiphysics 3.4 Software Package (Stockholm, Sweden). The 2D FEM was used to analyze the build-up of the thermal residual stresses within the proposed EBC layers during service condition. The modelling was based on three-node elements and a fine mesh through both the coating layer and the substrate interface. Models 1, 2 and 3 meshes consist of 51392, 35744 and 37920 elements, respectively as shown in Table 1 for the three different EBC model dimensions used. Each model consists of the same three sub layers but different thicknesses. The thicknesses of the distinct layers were varied to investigate its effects on the thermal residual stresses under service conditions. The width of each model was 6 mm.

The physical, thermal, and mechanical properties of the candidate coating layers and the substrate are presented in Table 2. The boundary condition was chosen such that, there was no displacement in x-direction for the bottom of the substrate. Thermal boundary conditions' effects were imitated by applying a temperature of 1500°C to the top layer and 25°C to the bottom part of the SiC/SiC CMC. Internal thermal boundaries between the layers of the thermo-mechanical models were set to continuity. Also, the left and right side of EBC system were thermally insulated in all the three models. Time-dependent analysis with linear analysis system solver was used for all the three models. Direct solution methods were considered in the FEM, because it is faster than iterative methods, and it is always recommended for 2D built models.

### 3. Results and Discussion

The conventional EBC is made up of BSAS, Mullite and Silicon with BSAS as top coat[14]. Low melting silicon at temperatures > 1400 °C prevents its use at higher temperatures. Further, in water-vapor atmospheres, BSAS suffers significant recession via volatilization at temperatures beyond 1400°C.  $Y_2Si_2O_7$  was chosen because of its low volatility and low CTE that matches the CTE of  $Y_2Si_2O_7$  and its improved adherence to SiC. The material combination systems and their interfacial interactions are presented in detail in section 3.1 to 3.3.

#### 3.1. $Y_2Si_2O_7$ - (SiC/SiC) System

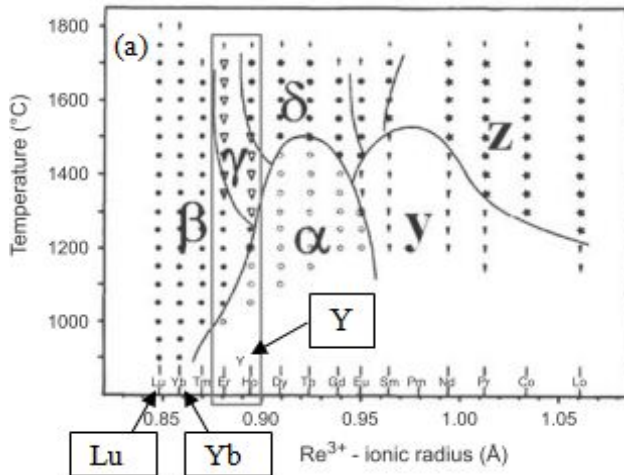


Figure 2. Phase diagram of rare earth disilicate polymorph[22, 23]

In the conventional design, silicon is used as bond coat due to its unique adherence to the SiC/SiC CMC. However, the use of silicon as a bond coat is limited by its melting point (~1416 °C). In air breathing engines that operate at temperatures greater than 1500°C, Si will melt leading to a significant reduction in service time of the EBC. In this work, Si was replaced by  $Y_2Si_2O_7$  which has a melting temperature of 1775°C [12, 20] and have similar CTE with SiC  $\sim 4 \times 10^{-6}/^\circ\text{C}$ . Therefore the use of  $Y_2Si_2O_7$  as a bond coat will

provide good adherence to the SiC/SiC CMC (Figure 3a).  $Y_2Si_2O_7$  has a low thermal conductivity of <3.0 W/mK above 300 °C and also, stable with  $SiO_2$  which is an oxidation product of SiC. This combination of properties suggests  $Y_2Si_2O_7$  as a possible bond coat with SiC/SiC CMCs.

#### 3.2. Mullite/ $Y_2Si_2O_7$ System

Mullite is selected as the intermediate layer due to its close CTE match with  $Y_2Si_2O_7$  hence may bond easily to mullite (Figure 3b). Also,  $Yb_2Si_2O_7$  has been shown to adhere to mullite[24]. Mullite is thermally stable up to 1890°C and is stable in dry and oxidizing atmospheres.



(a)



(b)



(c)

Figure 3. Structural schematic diagram (a)  $Y_2Si_2O_7$  (b)  $Y_2Si_2O_7$ /mullite (c)  $Y_2Si_2O_7$ /mullite/ $Yb_2Si_2O_7$  coatings system with SiC/SiC CMC

#### 3.3. $Yb_2Si_2O_7$ /Mullite System

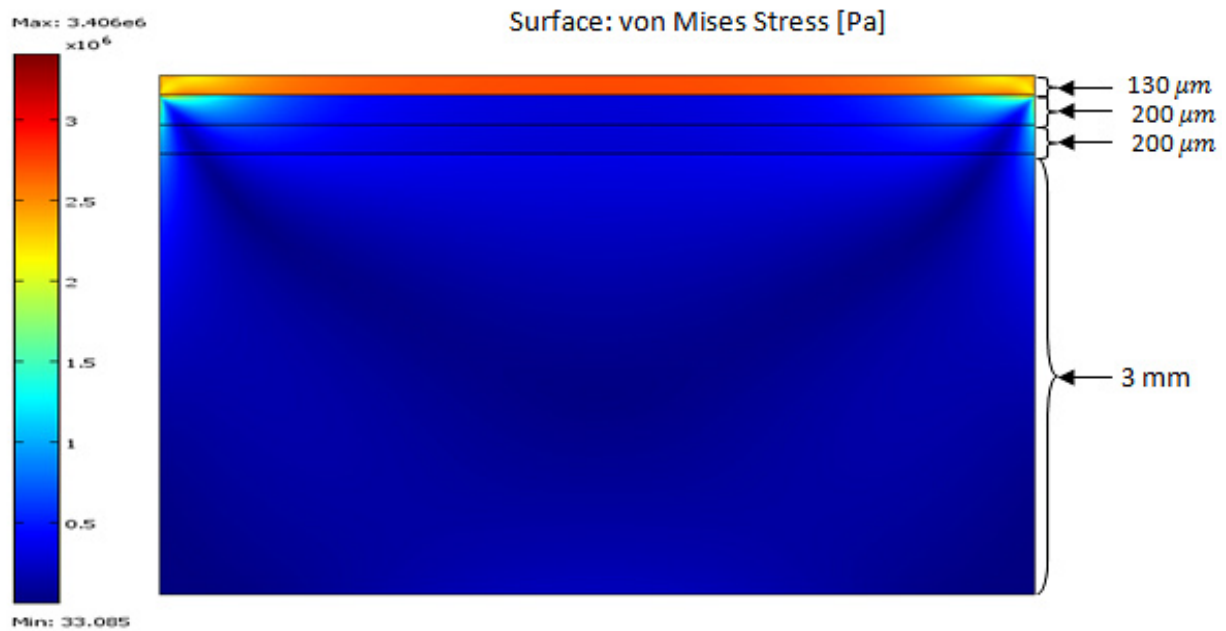
An oxide with low water-vapor volatility will serve as a good top coat on mullite, which has relatively high silica activity ( $\sim 0.3 - 0.4 \mu\text{m}/\text{h}$ ). High silica activity results in higher selective volatilization of silica and the recession of mullite[25]. Volatilization of silica from the mullite leads to a porous alumina and irregular cracks.[14]. A top coat of  $Yb_2Si_2O_7$  will protect the mullite interlayer from water vapor attack and subsequently mitigate its volatilization.  $Yb_2Si_2O_7$

is known to have a low recession rate than mullite[24]. Bansal et al. showed  $\text{Yb}_2\text{Si}_2\text{O}_7$  top coat on mullite to provide an EBC with no through thickness cracks.  $\text{Yb}_2\text{Si}_2\text{O}_7$  is thermally compatible with mullite and provides good adherence due to CTE ( $4 \times 10^{-6}/^\circ\text{C}$ ) match with mullite, CTE  $\sim 5 \times 10^{-6}/^\circ\text{C}$ . Further, advantage of the use of  $\text{Yb}_2\text{Si}_2\text{O}_7$  is that, it is thermally stable up to  $1850^\circ\text{C}$ . From the Rare earth disilicate polymorph phase diagram shown in figure 2, both Lu-silicates and Yb-silicates exhibit monoclinic phase stability up to  $1600^\circ\text{C}$ ; but due to significant higher cost of Lu, Yb was investigated more closely. Polymorphic rare earth disilicate materials vary in density and are not desirable coating candidates since volume change due to phase transformation[26] may cause cracks. The high melting temperature of  $\text{Yb}_2\text{Si}_2\text{O}_7$  ( $\sim 1850^\circ\text{C}$ ) makes it applicable in air breathing engines operating at temperatures of less than  $1500^\circ\text{C}$ .

### 3.4. Thermal Residual Stress Modelling Results

Figures 4a-c present the finite element analyses of the thermal residual stresses obtained for models 1, 2 and 3. The thermal load at the surface of all the three models is identical. Figure 6 shows the stresses within the EBC layers due to the surface thermal loading applied at  $1500^\circ\text{C}$  on both the coating and the substrate. It was observed that, the magnitude of thermal residual stresses within each layer is decreased when the thickness of the top coat increases. The smaller the thickness of the top coat, the higher the thermal gradient in the  $\text{Yb}_2\text{Si}_2\text{O}_7$  coating and as a result, a higher surface compressive stress was expected as reported by Choules et al., 2001[27] and Aziz et al., 2009[11]. Thermal residual stresses are generated in the EBC multilayered system due to differences in the thermal and elastic

properties of the underlying layers. Also, it was observed that, the thermal stress contribution in the coating was compressive while the substrate exhibited tensile thermal stress. This is as a result of difference between the substrate's (SiC/SiC) CTE and the EBC's CTE. The thickness of the  $\text{Yb}_2\text{Si}_2\text{O}_7$  top layer in model 1 is greater than the subsequent two coats. Comparing figures 4a, 4b and 4c show that, when the thickness of the top coat is small, the magnitude of thermal residual stresses within the layer is high. Since for all the three models, the CTE and elastic modulus mismatch between the underlying layers were the same, the difference in the thermal stresses were due to the difference in the thicknesses. It is very clear from Figure 4c that, the order of magnitude of the residual stresses is higher in model 3 than model 1 and 2. Comparing the three FEM results suggest that, model 1 has a better architecture in the proposed EBC system for SiC/SiC CMCs because the residual stresses are minimal. The lower the magnitude of the residual stresses, the greater the underlying coating can adhere. Analyzing the thermal residual stress within the individual layers of model 1 shows that, the maximum residual stress that exist between Mullite ( $200 \mu\text{m}$ ) and  $\text{Yb}_2\text{Si}_2\text{O}_7$  ( $130 \mu\text{m}$ ) (Figure 4d) is  $2.997 \times 10^6$  Pa. This maximum stress exist more in the  $\text{Yb}_2\text{Si}_2\text{O}_7$  ( $130 \mu\text{m}$ ) layer since it is exposed more to the thermal load ( $1500^\circ\text{C}$ ). Figure 4d shows that, the residual stress extend more into the mullite layer when mullite and  $\text{Yb}_2\text{Si}_2\text{O}_7$  are considered as compared with  $\text{Y}_2\text{Si}_2\text{O}_7$  ( $200$ ), Mullite ( $200$ ) and  $\text{Yb}_2\text{Si}_2\text{O}_7$  ( $130$ ). This is as a result of difference in composite CTE of the three layers and mullite layer. The stresses within  $\text{Y}_2\text{Si}_2\text{O}_7$  and SiC/SiC (Figure 4e) are relatively low, due to the massive reduction in the thermal load at  $\text{Y}_2\text{Si}_2\text{O}_7$  surface.



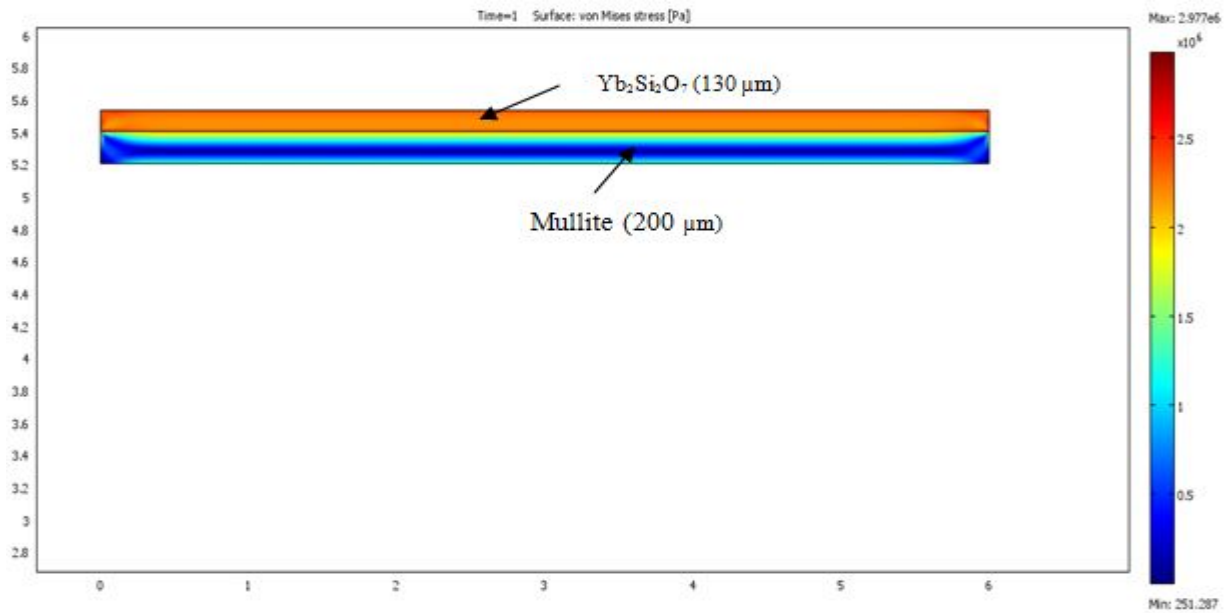
(a)



(b)



(c)



(d)



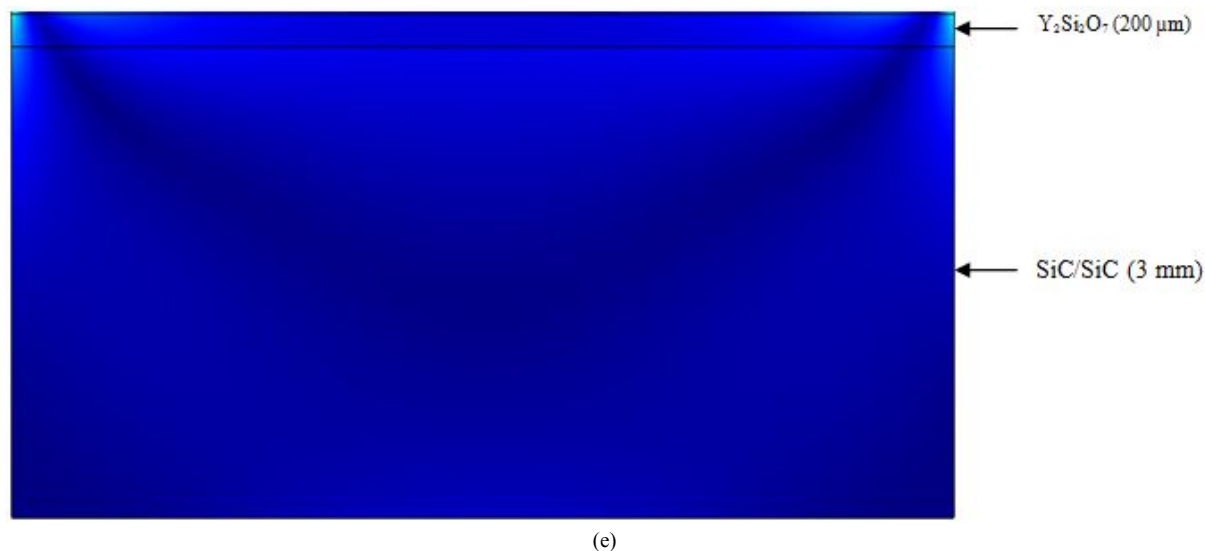


**Figure 4a-e.** presents the FEM for different EBC architecture and thicknesses; (a) Model 1:  $Y_2Si_2O_7$  (200), Mullite (200) and  $Yb_2Si_2O_7$  (130); (b) Model 2:  $Y_2Si_2O_7$  (200), Mullite (200) and  $Yb_2Si_2O_7$  (130) (c) Model 3:  $Y_2Si_2O_7$  (200), Mullite (200) and  $Yb_2Si_2O_7$  (130) with the SiC/SiC substrate. (d) Residual stress distribution within only Mullite (200) and  $Yb_2Si_2O_7$  (130) and (e) Residual stress distribution within only the  $Y_2Si_2O_7$  (200) and SiC/SiC substrate (3mm)

## 4. Conclusions

In this study, a novel EBC system for SiC/SiC CMCs applicable for use in air breathing engines was designed and the thermal residual stresses within the system were modelled to determine the optimum layer thickness. Three-layer EBC system was chosen based on the following factors: (i) Environmental stability, especially water vapour (ii) CTE match; (iii) Chemical compatibility; and (iv) Phase stability. Based on these requirements, the following three-layer coatings were recommended; namely:  $Y_2Si_2O_7$  (bond coat),  $3Al_2O_3 \cdot 2SiO_2$  (interlayer) and  $Yb_2Si_2O_7$  (top coat). The design indicates that, when Si bond coat is replaced by  $Y_2Si_2O_7$ , the EBC system function in air breathing engine at temperature ( $\sim 1500^\circ C$ ) because,  $Y_2Si_2O_7$  melts at  $\sim 1775^\circ C$  and Si melts at  $\sim 1416^\circ C$  respectively.

The thermal residual stresses within the proposed three multilayers models with SiC/SiC substrate during service condition were modeled using COMSOL Multiphysics 3.4. The FEM results show that, the thermal residual stress within the top layer decreased when the layer thickness was increased. The thermal residual stresses in the coating decreased as the thickness of the top coat increased.

## ACKNOWLEDGEMENTS

The authors are grateful to the Department of Materials Science and Engineering of the African University of Science and Technology (AUST) for funding this research.

## REFERENCES

- [1] Jacobson, N. S., Opila, E. J. and Lee, K. N., "Oxidation and Corrosion of Ceramics and Ceramic Matrix Composites," *Current Opinion in Solid State and Materials Science* 5, 301–309, 2001.
- [2] K.N. Lee, D.S. Fox, J.I. Eldridge, D. Zhu, R.C. Robinson, N.P. Bansal and R.A. Miller. "Upper Temperature Limit of Environmental Barrier Coating Based on Mullite and BSAS," *J. Am. Ceram. Soc.* 86[8] 1299-306, 2003.
- [3] Lee, K.N., Fox, D.S., Robinson R.C. and Bansal, N.P., "Environmental Barrier coatings for Silicon-based Ceramics, High Temperature Ceramic matrix Composite," Krenkel, W., Naslain, R. and Schneider, H. (eds), *High temperature ceramic matrix composites*. Weinheim, Germany: Wiley-VCH, pp. 224–229, 2001.
- [4] UK Patent no. 2427201, "Thermal / Environmental Barrier Coating System for Silicon-containing metals", 2013.
- [5] K.N. Lee, D.S. Fox and N.P. Bansal, "Rare Earth Environmental Barrier Coatings for SiC/SiC Composites and  $Si_3N_4$  Ceramics," *J. Eur. Ceram. Soc.*, 25(10): 1705–1715, 2005.
- [6] N.P. Bansal, J.P. Singh, W.M. Kriven and H. Schneider, "Advances in Ceramic Matrix Composites IX," *J. Am. Ceram. Soc.*, Vol. 153, pp. 331–343, 2003.
- [7] D.M. Zhu, R.A. Miller and D.S. Fox, "Thermal and Environmental Barrier Coating Development for Advanced Propulsion Engine Systems. NASA TM-2008-215040, Jan., 2008.
- [8] A. Abdul-Aziz and R.T. Bhatt, "Modeling of Thermal Residual Stress in Environmental Barrier Coated Fiber Reinforced Ceramic Matrix Composite," *Journal of composite materials*, 0(0) 1-8, 2011.
- [9] H.E. Eaton and G.D. Linsey, "Acceleration Oxidation of SiC CMC's By Water Vapor and Protection via Environmental Barrier Coating Approach," *J. Eur. Ceram. Soc.*, 22:2741, 2002.
- [10] S. Uenoa, T. Ohji and H. Lin, "Corrosion and Recession of

- Mullite in Water Vapor Environment,” *J. Eur. Ceram. Soc.*, 28:431, 2008
- [11] K.N. Lee, J.I. Eldridge and R.C. Robinson, “Residual Stresses and their Effects on the Durability of Environment Barrier Coatings for SiC Ceramics,” *J. Eur. Ceram. Soc.*, 88(12): 3483, 2005.
- [12] Z. Sun, Y. Zhou, J. Wang and M. Li, “ $\gamma$ - $Y_2Si_2O_7$ , a Machinable Silicate Ceramic: Mechanical Properties and Machinability,” *J. Am. Ceram. Soc.*, 90, 2535–41, 2007.
- [13] Z. Sun, L.Wu, M. Li, Y. Zhou, “Tribological Properties of  $\gamma$ - $Y_2Si_2O_7$  Ceramic against AISI 52100 Steel and  $Si_3N_4$  Ceramic Counterparts,” *Wear*, 266 960–967, 2009.
- [14] B. J. Harder, J.D. Almer, C.M. Weyant, K.N. Lee and K.T. Faber, “Residual Stress Analysis of Multilayer Environmental Barrier Coatings,” *J. Am. Ceram. Soc.*, 92[2] 452–459, 2009.
- [15] H. Samadi, “A Thick Multilayer Thermal Barrier Coating: Design, Deposition, and Internal Stresses,” Dept. of Materials Science and Engineering, *University of Toronto*. PhD thesis, 2009.
- [16] Y.R. Takeuchi and K. Kokini, “Thermal Fracture of Multilayer Ceramic Thermal Barrier Coatings, *Journal of Engineering for Gas Turbines and Power-Transactions of the ASME*, 1994, 116, p. 266-271.
- [17] Z. Sun, M. Li, and Y. Zhou, “Thermal properties of single phase  $Y_2SiO_5$ ,” *Journal of the European Ceramic Society* 29 551–557, 2009.
- [18] C. M. Toohey, “Novel Environmental Barrier Coatings for Resistance against Degradation by Molten, Glassy Deposits in the Presence of Water Vapor,” *Ohio State University*, Masters Thesis, 2011.
- [19] International Town Meeting on SiC/SiC Design and Material Issues for Fusion Systems Oak Ridge, January 18-19, 2000.
- [20] A.I. Becerro and A. Escudero, “Polymorphism in the  $Lu_{2-x}Y_xSi_2O_7$  System at High Temperatures,” *J. Eur. Ceram. Soc.*, 26. 2293–9. 2006.
- [21] D.M. Cupid and H. J. Seifert, “Thermodynamic Calculations and Phase Stabilities in the Y–Si–O System,” *J. Phase Equilib. Diff.*, 28, 90–100. 2007.
- [22] J. Felsche, “Polymorphism and Crystal Data of the Rare-Earth Disilicates of Type  $RE_2Si_2O_7$ ,” *J. Less Common Met.*, 21, 1–14. 1970.
- [23] J. Felsche, “The Crystal Chemistry of Rare-Earth Silicates,” *Struct. Bonding*, 13, 99–113. 1973.
- [24] K.N. Lee, “Current Status of Environmental Barrier Coatings for Si-based Ceramics,” *Surface and Coatings Technology*, 133-134, 1-7. 2000.
- [25] K. N. Lee, *Transactions of the ASME* 122 (2000): 632-636.
- [26] X. Yue, and Y. Zhaotong, “Investigation on the Preparation of Si/mullite/ $Yb_2Si_2O_7$  Environmental Barrier Coatings onto Silicon Carbide,” *Journal of Rare Earths*, Vol. 28, No. 3, p. 399. Jun. 2010.
- [27] B. D. Choules, K. Kokini and T.A Taylor, “Thermal fracture of ceramic thermal barrier coatings under high heat flux with time-dependent behaviour,” *Materials Science and Engineering a-Structural Materials Properties Microstructure and Processing*, 2001, 299, p. 96-304.